Synthesis, Spectroscopic Analysis, Biological Evaluation, and In Silico Studies of Novel Benzenesulfonate-Derived Schiff-Mannich Bases

[1]Ahmet Harmankaya, [2]Namık Kılınç, [1]Murat Beytur*, [1]Yonca Yılmaz, [1]Sevda Manap and [1]Haydar Yüksek

[1]*Department of Chemistry, Faculty of Science and Letters, Kafkas University, Kars 36100, Turkey.*
[2]*Department of Medical Services and Techniques, Vocational School of Health Services, Iğdır University, Iğdır, 76100, Turkey.*
muratbeytur83@gmail.com*

Summary: In the current study, 3-formyl phenyl benzenesulfonate is created by reacting 3-hydroxybenzaldehyde with benzene sulfonyl chloride, which is aided by triethylamine. Nine unique (Z)-3-[(3-substituted-5-oxo-1,5-dihydro-4H-1,2,4-triazol-4-yl)-iminomethyl] compounds were formed through the reaction of a manufactured 3-formyl phenyl benzenesulfonate chemical with nine 3-alkyl(aryl)-4-amino-4,5-dihydro-1H-1,2,4-triazol-5-one, as detailed in the existing literature. Phenyl benzene sulfonate (S) compounds were purchased. Through the reaction of the Schiff bases that were made a secondary amine, such as morpholine with formaldehyde, heterocyclic Mannich bases of a unique kind were created. Five recently found (Z)-3-[(3-substituted-5-oxo-1,5-dihydro-4H-1,2,4-triazol-4-yl)-iminomethyl] compounds are presented in this work. By reacting phenyl benzene sulfonate (S) with morpholine in the presence of formaldehyde, five new (Z)-3-[(3-substituted-1-(morpholinomethyl)-5-oxo-1,5-dihydro-4H-1,2,4-triazol-4-yl)-iminomethyl] compounds were created. Chemical compounds fall under the category of phenylbenzene sulfonates (M). Utilizing IR, ^{1}H NMR, and ^{13}C NMR spectroscopy, fourteen recently novel compounds' chemical structures were examined. The ability of the freshly synthesized Schiff and morpholine-derived Mannich bases to obstruct the aldose reductase enzyme's (AR) activity was also assessed. The 1,2,4-triazole functional group was modified by adding various groups at the 1 and 3 positions, resulting in a collection of compounds (S1–9 and M1, 2, 4, 5, 7). It was determined whether these synthetic compounds could prevent the human recombinant AR enzyme from working in vitro, and the findings were validated using molecular docking, molecular mechanics, and ADME analyses. To better understand this mechanism, synthetic Schiff and Mannich base derivatives as well as the positive control substance quercetin were tested using molecular docking against the human recombinant AR enzyme in vitro. To assess the drug-like properties of Schiff and Mannich base analogs, a series of absorption, distribution, metabolism, and excretion (ADME) properties were analyzed theoretically.

Keywords: Benzenesulfonate; Schiff base; Mannich Bases; 1,2,4-Triazole ring, Inhibitory activity; Docking Study.

Introduction

It has been noted that substances having a heterocyclic structure comprising a 1,2,4-triazole skeleton have the potential to have biological effects [1–10]. The capacity to demonstrate numerous chemical and biological applications is made easier by their structural variety [11–14]. Heterocyclic structures make for over 70% of the medications now on the market, with nitrogen or sulfur accounting for about 60% of these structural frameworks [15]. The 1,2,4-triazole derivatives have been linked to a few pharmacological effects, such as antibacterial [16,17], anti-inflammatory [18], analgesic [19], anti-cancer [20], and antioxidant characteristics [21,22]. Some of the current medications, including ribavirin (an antiviral agent) [23], rizatriptan (an antimigraine agent) [24], alprazolam (an anxiolytic agent) [25], and itraconazole (an antifungal agent) [26], are the best examples of possible molecules with a triazole ring and serve as examples of these pharmacological activities. Antibacterial [28], antifungal [29], anticancer [30], antimalarial [31], antimycobacterial [32], and antioxidant [33] properties of Mannich bases. Significant biological activity has been found in numerous fields of study in the past, particularly in medicine and medication development [1, 2]. Consequently, this class of heterocyclic compounds is receiving more attention.

Hyperglycemia, a pervasive and complex metabolic condition, is a hallmark of diabetes mellitus. The condition mentioned above has a sizable global frequency and has a substantial effect on people's general well-being. The pathological condition of hyperglycemia is defined by a significant amount of glucose being diverted into the polyol pathway. This is frequently regarded as the primary factor in the development of long-term diabetes complications, such as nephropathy, retinopathy, cataracts, and

---

*To whom all correspondence should be addressed.

neuropathy [34–36]. The aldo-keto reductase superfamily includes aldose reductase (ALR2, EC 1.1.1.21) [37, 38]. The enzyme responsible for catalyzing the NADPH-dependent reduction of glucose to sorbitol in the polyol pathway step that greatly affects the reaction rate is aldose reductase. A NAD+-dependent enzyme called sorbitol dehydrogenase then converts sorbitol into fructose. Sorbitol production that is excessive, an imbalance between the cofactors NAD+/NADH and NADPH/NADP+, and oxidative stress within the cells are all thought to be the main contributors to the cellular damage that results in problems from diabetes. In addition, increased concentrations of glycating agents, such as dihydroxyacetone phosphate, fructose, methylglyoxal (produced from fatty acid oxidation and increased glycolytic flux), and glyceraldehyde-3-phosphate, encourage the formation of advanced glycation end products (AGEs) within the cells. Reactive oxygen species (ROS) breeding may increase as a result of pathogenic alterations in intracellular protein activity brought on by AGEs. Protein kinase C (PKC) can be inappropriately activated during the conversion of dihydroxyacetone phosphate to diacylglycerol, which heightens oxidative stress [39].

The correlation between the development of long-term diabetic complications and aldose reductase (AR) has been substantiated by increasing research and evidence. As a result, inhibiting AR is a promising approach for preventing and delaying the onset of diabetes complications [40]. Studies have demonstrated that AR inhibitors (ARIs) have the potential to impede or postpone the progression of specific DM-related ailments in both animal models and human subjects [41–43].

Despite identifying a considerable number of Acute Respiratory Infections (ARIs) over the last three decades, clinical trials have often produced unsatisfactory results due to issues related to pharmacokinetics, adverse side effects, or inadequate in-vivo effect. Epalrestat is presently the sole ARI sanctioned for treatment, but distinct another inhibitors, as fidarestat, are undergoing clinical trials [34,44–46]. In general, Acute Respiratory Infections (ARIs) have the potential to offer innovative therapeutic alternatives for a range of ailments, such as sepsis, rheumatoid arthritis, uveitis, asthma, and atherosclerosis, as well as diabetes mellitus and its associated outcomes [47, 48].

In our latest work, 14 newly synthesized 3-substituted and 1-substituted 1,2,4-triazole derivatives were created. There was an effort made to clarify the structures of the produced heterocyclic compounds.

The investigation involves performing silico molecular docking analysis and in vitro biological activity experiments [1-3, 13, 49]. The 3-[(3-substituted-1-(H/morpholine)-5-oxo-1,5-dihydro-4H-1,2,4-triazole-4-yl)-iminomethyl]-phenyl benzene sulfonate was synthesized in this study along with a total of fourteen novel derivatives. Through the use of synthetic chemicals, the current study examined the human recombinant AR enzyme's in vitro effectiveness. In the current study, molecular docking was used to clarify the mechanism of action of quercetin, a positive control substance, on the human recombinant AR enzyme in an in vitro environment. To evaluate the drug-like characteristics of Schiff and Mannich Base derivatives, a number of ADME tests were conducted.

Experimental

Chemistry

All chemicals have been provided from Merck, Aldrich, and Fluka. The melting points of the synthesized newly compounds were determined using the Stuart SMP30 brand instrument for melting point determination. The collection of IR spectra to determine the structural details of compounds was facilitated by utilizing the ALPHA-P BRUKER FTIR spectrometer.

The 400 MHz NMR instrument on the BRUKER ULTRASHIELD PLUS BIOSPIN spectrometer was used to record the NMR spectra for ^{1}H and ^{13}C. Tetramethylsilane was used as the reference standard, and the solvent was used deuterated DMSO. There are six types of proton coupling patterns: single (s), double (d), triple (t), quartet (q), sextet (sext) and multiple (m). Parts per million (ppm) were used to measure the chemical changes in relation to the downstream compound tetramethylsilane. In the course of the inquiry, the initial compounds T and B were prepared using the literature sources [50, 51].

General Procedure for the Synthesis of (Z)-3-[(3-substitued-5-oxo-1,5-dihydro-4H-1,2,4-triazol-4-yl)-iminomethyl]-phenyl benzene sulfonate (S1-9)

This study represents the initial synthesis of nine 3-alkyl(aryl)-4-amino-4,5-dihydro-1H-1,2,4-triazol-5-one (T1-9) molecules required for this investigation. The present study investigated the reactions of various substances with 3-formyl phenyl benzenesulfonate, synthesized from the reaction of 3-hydroxybenzaldehyde (10 mmol) with benzene sulfonyl chloride (10 mmol), using triethylamine as a

catalyst. As a result, nine novel (Z)-3-[(3-substitued-5-oxo-1,5-dihydro-4H-1,2,4-triazol-4-yl)-iminomethyl]-phenyl benzene sulfonate (S1-9) were synthesized (Scheme 1). Spectroscopic analyses techniques such as IR, ^{1}H-NMR, and ^{13}C-NMR were employed to identify the novel compounds produced in the study (Table 1, 3, 5 and 7).

General procedure for newly synthesized Mannich Bases compounds (M1, 2, 4, 5, 7)

a Solution of 100 mL ethanol was prepared independently for each of the five unique 3-(Z)-3-[(3-substituted-5-oxo-1,5-dihydro-4H-1,2,4-triazol-4-yl)-

iminomethyl]-phenyl benzene sulfonates (S1, 2, 4, 5, and 7). The solutions were subjected to reflux for three hours after combining morphine (10 mmol) and a 37% formaldehyde solution (20 mmol), followed by heating. The white crystals obtained were subjected to multiple rounds of crystallization in ethanol and subsequently dried under vacuum conditions to yield (Z)-3-[(3-substituted-1-(morpholinomethyl)-5-oxo-1,5-dihydro-4H-1,2,4-triazol-4-yl)-iminomethyl]-phenyl benzene sulfonates (M1, 2, 4, 5 and 7), individually. Spectroscopic analyses techniques such as IR, ^{1}H-NMR, and ^{13}C-NMR were employed to identify the novel compounds produced in the study (Table 2, 4, 6 and 8).

Table-1: Substituted groups, phases, yields and melting point values of S type compounds.

Compound	3-Substitue	phase	Yield (%)	Melting Point (°C)
S1	Methyl	White needles	97	206
S2	Ethyl	White needles	98	178
S3	n-Propyl	White needles	96	162
S4	Benzyl	White needles	98	152
S5	p-Methylbenzyl	White needles	98	177
S6	p-Methoxybenzyl	White needles	93	174
S7	p-Chlorobenzyl	White needles	98	202
S8	p-Chlorobenzyl	White needles	96	149
S9	Phenyl	White needles	98	146

Table-2: Substituted groups, phases, yields and melting point values of M type compounds.

Compound	3-Substitute	Structure	Yield (%)	Melting Point (°C)
M1	*Methyl*	White needles	71	131
M2	*Ethyl*	White needles	79	The Charred
M4	*Benzyl*	White needles	78	102
M5	*p-Methylbenzyl*	White needles	80	98
M7	*p-Chlorobenzyl*	White needles	80	122

Table-3: IR values of S type compounds (cm^{-1}).

Compound	NH	C=O	C=N	1,4-Disubstituted aromatic ring	1,3-Disubstituted aromatic ring	Monosubstituted aromatic ring
S1	3165	1696	1606		799 and 733	
S2	3163	1704	1598		799 and 683	
S3	3182	1703	1591		800 and 717	
S4	3189	1701	1572		795 and 727	756 and 679
S5	3155	1701	1612	830	786 and 711	
S6	3153	1696	1608	828	786 and 713	
S7	3172	1703	1572	841	798 and 722	
S8	3168	1709	1573		788 and 719	
S9	3171	1699	1609		803 and 720	762 and 641

Table-4: IR values of M type compounds (cm^{-1}).

Compound	C=O	C=N	1,4-Disubstituted aromatic ring	1,3-Disubstituted aromatic ring
M1	1702	1611		793 and 715
M2	1697	1608		807 and 731
M4	1690	1607	839	796 and 736
M5	1697	1607	830	801 and 735
M7	1696	1572	827	800 and 735

Table-5: ^{1}H-NMR values of S type compounds (^{1}H-NMR (400 MHz, DMSO-d$_6$, ppm).

Comp.	NH	N=CH	ArH	C3-ArH	C3-Alkyl-H
S1	11.85 (s, 1H)	9.68 (s, 1H)	7.91 (d, 2H), 7.76 (d, 1H), 7.69 (t, 2H), 7.52 (t, 1H), 7.44 (s, 1H, ArH), 7.19 (dd, 1H)		2.23 (s, 3H, CH$_3$)
S2	11.87 (s, 1H)	9.68 (s, 1H)	7.90 (dd, 2H), 7.84 (t, 1H), 7.76 (d, 1H), 7.69 (t, 2H), 7.53 (t, 1H), 7.42 (s, 1H), 7.21 (dd, 1H)		2.61 (q, 2H, CH$_2$), 1.19 (t, 3H, CH$_3$)
S3	11.88 (s, 1H)	9.68 (s, 1H)	7.90 (dd, 2H), 7.84 (t, 1H), 7.75 (d, 1H), 7.69 (t, 2H), 7.53 (t, 1H), 7.43 (s, 1H), 7.21 (dd, 1H)		2.58 (t, 2H, CH$_2$), 1.65 (sext, 2H, CH$_2$), 0.95 (t, 3H, CH$_3$)
S4	12.01 (s, 1H)	9.65 (s, 1H)	7.90 (d, 2H), 7.81 (t, 1H), 7.72-7.66 (m, 3H), 7.50 (t, 2H), 7.14 (d, 1H)	7.32-7.24 (m, 5H)	4.00 (s, 2H, CH$_2$Ph)

S5	11.98 (s, 1H)	9.64 (s, 1H)	7.91 (dd, 2H), 7.81 (t, 1H), 7.73-7.66 (m, 3H), 7.50 (t, 2H), 7.14 (d, 1H)	7.18-7.14 (m, 4H)	3.94 (s, 2H, CH₂Ph), 2.25 (s, 3H, PhCH₃)	
S6	11.97 (s, 1H)	9.64 (s, 1H)	7.91 (dd, 2H), 7.81 (t, 1H), 7.73 (d, 1H), 7.68 (t, 2H), 7.51 (t, 2H), 7.14 (dd, 1H)	7.20 (d, 2H), 6.87 (d, 2H)	3.92 (s, 2H, CH₂Ph), 3.71 (s, 3H, PhOCH₃)	

Table Continue

S7	12.02 (s, 1H)	9.65 (s, 1H)	7.90 (d, 2H), 7.81 (t, 1H), 7.72 (d, 1H), 7.68 (t, 2H), 7.50 (t, 2H), 7.15 (dd, 1H)	7.37 (d, 2H), 7.32 (d, 2H)	4.02 (s, 2H, CH₂Ph)	
S8	12.03 (s, 1H)	9.65 (s, 1H)	7.90 (dd, 2H), 7.81 (td, 1H), 7.73 (d, 1H), 7.67 (t, 2H), 7.50 (t, 2H), 7.16 (dd, 1H)	7.26-737 (m, 4H)	4.04 (s, 2H, CH₂Ph)	
S9	12.41 (s, 1H)	9.67 (s, 1H)	7.84-7.90 (m, 4H), 7.68 (t, 2H), 7.64 (t, 2H), 7.18 (dd, 1H)	7.50-7.56 (m, 5H)		

Table-6: ^{1}H-NMR values of M type compounds (^{1}H-NMR (400 MHz, DMSO-d$_6$, ppm).

Comp.	N=CH	ArH	C3-ArH	NCH₂N	Morpholine CH₂OCH₂	Morpholine CH₂NCH₂	C3-Alkyl-H
M1	9.77 (s, 1H)	7.86 (dd, 2H), 7.69 (t, 1H), 7.62 (d, 1H), 7.55 (t, 1H), 7.42 (s, 1H), 7.38 (t, 1H), 7.26 (s, 1H), 7.10 (dd, 1H)		4.61 (s, 2H)	3.71 (t, 4H)	2.71 (t, 4H)	2.34 (s, 3H, CH₃
M2	9.76 (s, 1H)	7.86 (dd, 2H), 7.69 (t, 1H), 7.62 (d, 1H), 7.55 (t, 1H), 7.40 (s, 1H), 7.38 (t, 1H), 7.28 (s, 1), 7.11 (dd, 1H)		4.62 (s, 2H)	3.70-3.72 (m, 4H)	2.70-2.74 (m, 4H)	2.70-2.74 (m, 2H, CH₂CH₃), 1.29 (t, 3H, CH₂CH₃)
M4	9.70 (s, 1H)	7.86 (d, 2H), 7.66 (t, 1H), 7.51-7.55 (m, 3H), 7.44 (s, 1H), 7.26 (s, 1H), 7.05 (dd, 1H)	7.31-7.34 (m, 5H)	4.65 (s, 2H)	3.72 (t, 4H)	2.72 (t, 4H)	4.05 (s, 2H, CH₂Ph)
M5	9.70 (s, 1H)	7.86 (dd, 2H), 7.66 (t, 1H), 7.56-7.51 (m, 2H), 7.44 (s, 1H), 7.35 (t, 1H), 7.26 (s, 1H), 7.06 (dd, 1H)	7.21 (d, 2H), 7.13 (d, 2H)	4.64 (s, 2H)	3.72 (t, 4H)	2.72 (t, 4H)	4.00 (s, 2H, CH₂Ph), 2.32 (s, 3H, PhCH₃)
M7	9.72 (s, 1H)	7.86 (d, 2H), 7.67 (t, 1H), 7.50-7.56 (m, 3H), 7.35 (t, 1H), 7.26-7.32 (m, 1H) 7.04 (dd, 1H)	7.50-7.56 (m, 1H), 7.35 (t, 1H) 7.26-7.32 (m, 3H)	4.65 (s, 2H)	3.72 (t, 4H)	2.71 (t, 4H)	4.03 (s, 2H, CH₂Ph)

Table-7. ^{13}C-NMR values of S type compounds (^{13}C-NMR (100 MHz, DMSO-d$_6$, ppm)

Comp.	Triazole-C₅	N=CH	Triazole-C₃	ArC	C3-ArC	C3-Alkyl-C
S1	151.62	151.08	144.22	149.40, 135.63, 135.15, 134.21, 130.78, 129.86 (2C), 128.26 (2C), 127.32, 124.80, 119.91		11.00 (CH₃)
S2	151.60	151.22	147.99	149.42 135.66, 135.13, 134.21, 130.82, 129.85 (2C), 128.24 (2C), 127.40, 124.86, 119.73		18.44 (CH₂), 10.02 (CH₃)
S3	151.63	151.17	146.84	149.42, 135.65, 135.12, 134.19, 130.82, 129.84 (2C), 128.23 (2C), 127.36, 124.85, 119.76		26.58 (CH₂), 18.86 (CH₂), 13.48 (CH₃)
S4	151.51	151.07	146.17	149.42, 135.63, 135.12, 134.22, 130.76, 129.86 (2C), 128.21 (2C), 127.40, 124.72, 119.98	135.65 128.77, 128.46 (2C), 126.76	31.08 (CH₂Ph)
S5	151.48	151.07	146.32	149.39, 135.65, 135.12, 134.21, 130.77, 129.86 (2C), 128.21 (2C), 127.40, 124.70, 119.97	135.82, 132.53, 129.02 (2C), 128.64 (2C)	30.68 (CH₂Ph), 20.59 (CH₃)
S6	151.45	151.02	146.47	149.39, 135.66, 135.12, 134.21, 130.78, 129.86 (2C), 128.21 (2C), 127.41, 124.71, 119.99	158.12, 129.75, 128.09, 113.90 (2C), 113.79	55.01 (PhOCH₃), 30.23 (CH₂Ph)
S7	151.63	151.05	145.83	149.38, 135.58, 135.11, 134.22, 130.78, 129.85 (2C), 128.22 (2C), 127.36, 124.74, 120.06	135,58, 131.47, 130.71 (2C), 128.39 (2C)	30.39 (CH₂Ph)
S8	151.70	151.03	145.65	149.40, 135.57, 135.11, 134.22, 130.75, 129.84 (2C), 128.22 (2C), 127.25, 124.76, 120.18	138.02, 132.99, 130.27, 128.80, 127.61, 126.82	30.63 (CH₂Ph)
S9	154.15	151.22	144.57	149.40, 135.49, 135.11, 134.10, 130.88, 129.82 (2C), 128.16 (2C), 127.29, 124.91, 120.31	130.18, 128.51 (2C), 127.97 (2C), 126.48	

Table-8: ^{13}C-NMR values of M type compounds (^{13}C-NMR (100 MHz, DMSO-d$_6$, ppm).

Comp.	Triazole-C₅	N=CH	Triazole-C₃	ArC	C3-ArC	Morpholine OCH₂	NCH₂N	Morpholine NCH₂	C3-Alkyl-C
M1	152.07	150.98	143.84	150.06, 135.78, 135.41, 134.37, 130.13, 129.24 (2C), 128.52 (2C), 127.03, 125.08, 120.84		66.81 (2C)	66.62	50.46 (2C)	11.34 (CH₃)
M2	151.99	151.13	147.75	150.06, 135.84, 135.36, 134.37, 130.14, 129.23 (2C), 128.50 (2C), 127.01, 125.06, 120.74		66.81 (2C)	66.57	50.42 (2C)	19.04 (CH₂CH₃), 10.43 (CH₂CH₃)
M4	151.97	151.01	145.62	150.05, 135.42, 135.09, 134.38, 130.09, 129.25 (2C), 128.75 (2C), 127.18, 124.94, 120.78	135.81, 128.87 (2C), 128.47 (2C), 127.09	66.85 (2C)	66.72	50.46 (2C)	31.82 (CH₂Ph)
M5	151.92	151.02	145.82	150.05, 135.65, 135.43, 134.38, 130.09, 129.44 (2C), 128.48 (2C), 127.08, 124.92, 120.79	136.82, 131.97, 129.25 (2C), 128.76 (2C)	66.85 (2C)	66.69	50.46 (2C)	31.38 (CH₂Ph), 21.04 (PhCH₃)
M7	152.16	150.95	145.18	150.06, 135.68, 135.38, 134.41, 130.15, 129.27 (2C), 128.47 (2C), 127.20, 124.98, 120.66	133.49, 133.15, 130.27 (2C), 128.93 (2C)	66.83 (2C)	66.75	50.45 (2C)	31.22 (CH₂Ph)

Aldose reductase activity assay and inhibition studies

A modified version of Cerelli's method for measuring enzyme activity was used to gauge the AR enzyme's activity. Using a 1 mL cuvette, the following components were added to measure the enzyme activity: 0.25 mL of Na-phosphate buffer, 0.45 mL of distilled water, 0.1 mL of NADPH, 0.1 mL of NADPH, 0.1 mL of enzyme solution, and 0.1 mL of DL-glyceraldehyde. Spectrophotometry was used to measure enzyme activity in order to find the decrease in NADPH concentration at 340 nm [52]. Enzyme inhibition experiments were carried out using the Optizen Pop UV/VIS spectrophotometer. The goal of the study was to determine whether the AR enzyme might be inhibited by the 3-[(3-substituted-1-(H/morpholine)-5-oxo-1,5-dihydro-4H-1,2,4-triazol-4-yl)-iminomethyl]-phenyl benzene sulfonate derivatives. The current investigation examined the inhibitory effects of each chemical at five different doses on the enzyme. The amount of enzyme activity in the control cuvette without inhibitors was taken to be 100%, and the inhibitor doses (IC50 values) that resulted in a 50% reduction in enzyme activity were calculated. The AR enzyme uses DL-glyceraldehyde as a substrate. The data on inhibition are shown in Table 2.

Molecular docking studies

1.08° resolution X-ray crystal structure of AR was discovered in the RCSB Protein Data Bank with the PDB code 2FZD. The crystal structure of the AR receptor was used to conduct molecular docking tests. For this purpose, the Small Drug Discovery Suites package (Schrodinger 2020-3, LLC, USA) was used. The Protein Preparation Wizard tool, available in Maestro 12.5, was used to build and repair the 3D crystal structure. The protein structure underwent hydrogen atom addition to correct any defects after bond order and charge were established [53]. The work of adding the missing side chains was completed using the Prime software. Under physiological pH circumstances, amino acids were ionized using the Propka software. Less than three interactions between a water molecule and a protein or ligand resulted in their elimination. Using the OPLS3e force field, energy minimization was then completed. Using Maestro 12.5 software, the process of creating three-dimensional (3D) structures for synthetic substances was carried out, and the 2D structures were sketched. Using Maestro 12.5's LigPrep module, ligands were converted into a three-dimensional (3D) structure. Epik module and OPLS3e force field were utilized to achieve accurate molecular geometries, and protonation states at a pH range of 7.0 ±2.0.

The Glide-Induced-Fit Docking (IFD) approach [54], as mentioned in our earlier study [2], was used to simulate molecular docking. Utilizing the re-docking process allows for the confirmation of the docking methodology. The co-crystal ligand TOL (Tolrestat) was isolated, and it underwent a similar re-docking procedure onto the homologous protein. After docking the co-crystal ligand, the Root Mean Square Deviation (RMSD) value was calculated using the Maestro Superposition Panel. When the resulting RMSD value is less than 2°, the validity of a docking procedure is proven [55].

Assessment of absorption, distribution, metabolism, and excretion (ADME)

Using Maestro 12.5, the QikProp module was used to carry out the ADME evaluation. The findings of the study shed light on the drug's pharmacokinetic properties, which include their absorption, distribution, metabolism, and elimination. Lipinski's rule of five, which considers factors like logPo/w, molecular weight, accptHB, and donorHB, was used to analyze the compounds' drug-likeness (QikProp, Schrödinger 2020-3, 2020).

Calculation of binding free energy using molecular mechanics/generalized born surface area (mm-gbsa)

The present study involved the determination of the electrostatic contribution of the VSGB solvation model, which was employed in conjunction with the OPLS3 force field. This was accomplished using MM-GBSA panel calculations, incorporating a Generalized Born Surface Area (GBSA) approach. The MM-GBSA approach employs molecular mechanics computations with continuum solvation models to evaluate macromolecules' binding free energies (Gbind) [56].
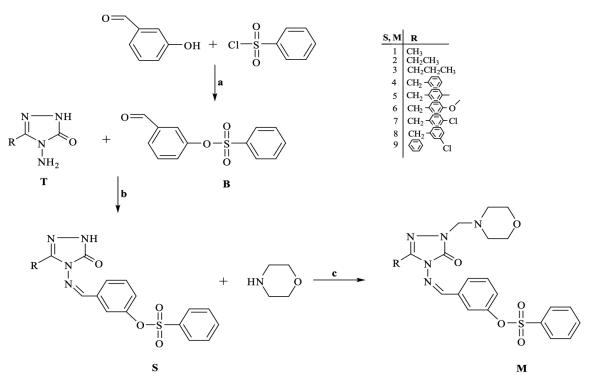
Results and Discussion

General steps for the synthesis of novel Schiff bases (S1-9) and Mannich bases (M1, 2, 4, 5, 7)

The objective of the current study was to synthesize new chemicals utilizing the synthetic process shown in Scheme 1. We are considering the literary work identified by the molecular nomenclature (Z)-3-[(3-substituted-5-oxo-1,5-dihydro-4H-1,2,4-triazol-4-yl)-iminomethyl]. In the current work, nine different 3-substituted-4-amino-4,5-dihydro-1H-1,2,4-triazole-5-ones (T1-9) were used to react with 3-formyl phenyl benzene sulfonate (B) to produce phenyl benzene sulfonate (S1-9) in an acetic acid

medium. The (Z)-3-[(3-substituted-5-oxo-1,5-dihydro-4H-1,2,4-triazol-4-yl)-iminomethyl] reacts with the morpholine. Five new (Z)-3-[(3-substituted-1-(morpholinomethyl)-5-oxo-1,5-dihydro-4H-1,2,4-triazol-4-yl)-iminomethyl] compounds were made using phenyl benzene sulfonate (S1-9) as a starting material and formaldehyde as the product. We received phenyl benzene sulfonates (M1, 2, 4, 5, 7).

Through the polyol pathway, the enzyme AR aids in the conversion of glucose to sorbitol, which is then changed into fructose by sorbitol dehydrogenase. Numerous diabetes problems, including retinopathy, nephropathy, cataracts, and neuropathy, have been linked to sorbitol buildup [57]. Nearly all human cells have the oxidoreductase enzyme AR, a critical part of the polyol pathway. Diabetes patients had higher levels of AR in their lenses, retinas, and sciatic nerves [58]. Increased flux in the lens fiber's polyol pathway might result in sorbitol accumulation, which facilitates water infiltration and the ensuing emergence of chronic diabetes problems. Therefore, controlling and avoiding these consequences requires decreasing androgen receptor (AR) activity. The onset of osmotic stress and the development of cataracts are both influenced by this process. Increased oxidative stress is associated with the pathogenesis of diabetes mellitus. Numerous aldose reductase inhibitors (ARIs) .

have been reported; however, due to the adverse effects they cause in patients, clinical licensing for these drugs has not yet been approved [59]. Therefore, employing bioactive substances with anti-androgenic characteristics is advantageous in both preventing and treating issues associated with diabetes. This study's goal was to investigate the pharmacological characteristics and AR-inhibitory effects of phenyl benzene sulfonate derivatives (S1-9 and M1, 2, 4, 5, 7) are [(3-substituted-1-(H/morpholine)-5-oxo-1,5-dihydro-4H-1,2,4-triazol-4-yl]-iminomethyl derivatives.

In this study, the newly synthesized derivatives of 3-[(3-substituted-1-(H/morpholine)-5-oxo-1,5-dihydro-4H-1,2,4-triazol-4-yl)-iminomethyl]-phenyl benzene sulfonate (**S1-9 and M1, 2, 4, 5, 7**) were evaluated for their potential to inhibit the human recombinant AR enzyme. The IC_{50} values of **S1-9, M1, M2, M4, M5, and M7** compounds were found to vary between 43.30 µM and 11.18 µM. (Z)-3-[(3-(p-Chlorobenzyl)-5-oxo-1,5-dihydro-4H-1,2,4-triazol-4-yl)-iminomethyl]-phenyl benzene sulfonate (**S7**) was found to be the most effective compound on human recombinant AR enzyme with an IC_{50} value of 11.18 µM (**Table 9**).

Scheme-1: Design of new target compounds. (a) Triethlamine, reflux, 3 h. (b) AcOH, reflux, 2h; (c) EtOH, HCHO, 3 h.

Table-9: In vitro inhibition results of 3-[(3-substituted-1-(H/morpholine)-5-oxo-1,5-dihydro-4H-1,2,4-triazole-4-yl)-iminomethyl]-phenyl benzene sulfonate derivatives.

Compound	IC$_{50}$ (µM)	R^2	Compound	IC$_{50}$ (µM)	R^2
S1	38.50 µM	0.97	M1	17.77 µM	0.96
S2	43.30 µM	0.98	M2	24.75 µM	0.98
S3	43.30 µM	0.95			
S4	19.80 µM	0.95	M4	34.65 µM	0.96
S5	16.10 µM	0.91	M5	19.80 µM	0.99
S6	15.06 µM	0.87			
S7	11.18 µM	0.94	M7	25.67 µM	0.97
S8	31.50 µM	0.92			
S9	33.00 µM	0.95			
Quercetin	5.68 µM	0.93			

The inhibitory mechanism of synthetic Schiff and Mannich Base derivatives and the positive control medication quercetin against the human recombinant AR enzyme was investigated in the current work using molecular docking in an in vitro context. The MM-GBSA method assessed the unbound binding energies of enzyme and inhibitor complexes. Table 10 lists the calculated docking scores and free binding energies that were acquired using the MM-GBSA and molecular docking techniques. Several ADME (absorption, distribution, metabolism, and excretion) experiments were used to gauge the drug-like qualities of Schiff and Mannich Base derivatives. (Table 11).

Table-10: Docking scores and free binding energy results of 3-[(3-substituted-1-(H/morpholine)-5-oxo-1,5-dihydro-4H-1,2,4-triazole-4-yl)-iminomethyl]-phenyl benzene sulfonate derivatives (S1-9 and M1, 2, 4, 5, 7) with AR enzyme

Compound	IFD Docking Score	MM-GBSA (ΔGbind)	Compound	IFD Docking Score	MM-GBSA (ΔGbind)
S1	-13.824	-58.81	M1	-13.538	-64.07
S2	-12.216	-57.24	M2	-12.465	-68.08
S3	-11.972	-42.75			
S4	-13.566	-58.86	M4	-11.107	-53.39
S5	-14.185	-56.90	M5	-12.956	-58.97
S6	-15.214	-53.95			
S7	-18.677	-58.97	M7	-13.473	-42.42
S8	-13.174	-58.97			
S9	-12.152	-63.17			
Quercetin	-14.480	-55.91			

Table-11: ADME prediction findings of newly synthesized 3-[(3-substituted-1-(H/morpholine)-5-oxo-1,5-dihydro-4H-1,2,4-triazole-4-yl)-iminomethyl]-phenyl benzene sulfonate derivatives (S1-9 and M1, 2, 4, 5, 7)

Name	mol MW	QP logPo/w	QPlogS	QPPCaco	QPlogBB	QPPMDCK	% HOA	Rule of Five	Rule of Three
M7	568.046	2.636	-0.769	321.91	-0.268	335.935	74.308	1	0
M5	547.628	2.784	-0.601	313.155	-0.39	156.969	74.958	1	0
M4	533.601	2.598	-1.04	347.271	-0.437	176.03	74.674	1	0
M2	471.530	1.607	-1.526	122.885	-0.961	57.011	73.756	0	0
M1	457.503	1.307	0.015	264.853	-0.381	130.187	77.968	0	0
S9	420.442	2.455	-2.702	139.986	-2.323	59.707	79.73	0	0
S8	468.914	2.946	-3.376	204.013	-1.266	149.957	85.535	0	0
S7	468.914	3.541	-4.364	217.743	-1.323	205.163	89.522	0	0
S6	464.495	3.711	-4.684	223.075	-1.617	100.633	90.709	0	0
S5	448.495	3.676	-5.736	110.305	-2.093	46.861	85.026	0	1
S4	434.469	2.918	-3.335	258.799	-1.315	118.916	87.22	0	0
S3	386.425	1.787	-2.647	92.279	-1.678	38.633	72.581	0	0
S2	372.398	1.928	-3.405	129.322	-1.692	55.733	76.026	0	0
S1	358.371	1.517	-3.204	169.003	-1.487	75.098	75.702	0	0
Quercetin	302.24	0.359	-2.886	18.196	-2.409	6.51	51.596	0	1
Recommended Range	130.0 – 725.0	–2.0 – 6.5	–6.5 – 0.5	<25 poor, >500 great	–3.0 – 1.2	<25 poor, >500 great	>80% is high <25% is poor	maximum is 4	maximum is 3

The 1,2,4-triazole functional moiety was modified by adding various groups at the 1 and 3 positions to produce a group of compounds (S1–9 and M1, 2, 4, 5, 7). Investigations were done in vitro to determine how the synthetic chemicals affected the inhibition of the human recombinant AR enzyme. Following that, the findings were confirmed using molecular docking, molecular mechanics, and ADME analyses. In a recent work, the in vitro inhibition of human recombinant AR enzyme was examined. The findings indicate that the AR enzyme is mildly inhibited

by the S1 compound, which features a methyl group attached to the 3 positions of the triazole ring with an IC$_{50}$ value of 38.5 µM. The **M1** compound demonstrated a significant inhibitory effect (IC$_{50}$= 17.77 µM) upon attachment of the morpholinomethyl group to the 1 position of the triazole ring in the **S1** compound. The experimental results are supported by the MM-GBSA free binding energies, which are shown in Table 2. Despite the absence of a clear distinction in docking scores between the two compounds in *in silico* research, these data support the experimental results. The

compound **S9**, which involves the attachment of a phenyl group to the 3 position of the triazole ring, exhibited a moderate inhibitory effect on the AR enzyme, as evidenced by its IC_{50} value of 33 µM. The S4 molecule, a triazole ring derivative with a phenyl group added at the 3 position, significantly inhibited the AR enzyme. The M4 molecule, a derivative of the identical triazole ring with a morpholinomethyl group attached at the 1 position, had a somewhat lesser inhibitory action, though. The results of the MM-GBSA free binding energy test and the docking scores, which are shown in Table 2, both support the experimentally determined difference in inhibition between the Schiff Base compound S4 and Mannich Base compound M4 for the AR enzyme. Comparing the inhibition activities of compound S2, which was created by adding an ethyl group to the triazole ring at position 3, and compound M2, which was created by adding an ethyl group to the triazole ring at position 3 and a morpholinomethyl group to the triazole ring at position 1, it was found that the binding of the morpholinomethyl group caused a significant increase in the inhibition activity of roughly 75%, as indicated. The results of the two compounds' docking scores and MM-GBSA free binding energies indicate that the M2 compound has a higher affinity for the AR enzyme than the other compound. Specifically, the compound **S2** ΔG_{bind} value was determined to be -57.24 kcal/mol, while the compound **M2** ΔG_{bind} value was found to be -68.08 kcal/mol. The compound denoted as **S5** was synthesized by introducing a methylbenzyl moiety at the third position of the triazole ring. This compound exhibits a potent inhibitory effect against the human recombinant AR enzyme, with an IC_{50} value of 16.1 µM. Additionally, it has been ascertained that **compound M2**'s inhibitory effect, resulting from the fusion of the morpholinomethyl group with the triazole ring at position 1 of **compound M7**, has undergone a reduction of approximately 23%. The primary cause for this discrepancy is that, while the **S5** compound engages in four π-π interactions with the activity center residues TRP20, VAL47, TYR48, and TYR209 of the AR enzyme through its methylphenyl functional group, the **M5** compound does not exhibit such interactions (**Figure 1A and B**). Among the synthesized compounds, **S7** exhibited the highest degree of inhibitory activity against the AR enzyme, owing to the attachment of a chlorobenzyl group to the 3 position of the triazole ring. The **S7** compound was subjected to in silico studies, demonstrating an inhibitory effect comparable to the positive control sample Quercetin. The IC_{50} value of the **S7** compound was determined to be 11.18 µM, and this finding agreed with the experimental results. Figures 1E and F show interactions between the chemical S7 and the active site of the AR enzyme that are similar to those of quercetin. Figure 2 shows that the S7

molecule created a halogen connection with the Cl group, whereas quercetin established a salt bridge interaction with the LYS77 residue. The AR enzyme was substantially less sensitive to the S8 derivative than the S7 compound, which was created by moving the Cl moiety from the 4th to the 3rd position of the S7 compound. The Cl moiety's new position prevented it from interacting with the LYS77 residue, which resulted in a significant drop in activity, as seen in Figure 1C. It follows that the LYS77 residue plays a significant role in inhibiting the AR enzyme via quercetin and the S7 molecule. Its effectiveness was decreased when the methoxy moiety formed the S6 molecule in place of the chlorine moiety that was in the fourth position of the S7 molecule. The HIS110 amino acid residue in the active site was seen to be hydrogen bound to the S6 compound, and the S6 compound was also seen to be interacting negatively with the TRP111 residue (Figure 1D).

The pharmacokinetics and drug-likeness of derivatives of 3-[(3-substituted-1-(H/morpholine)-5-oxo-1,5-dihydro-4H-1,2,4-triazol-4-yl)-iminomethyl]-phenyl benzene sulfonate were predicted using the Maestro QikProp tool.

The goal of the current study was to investigate the physiochemical and pharmacological properties of molecules generated by Schiff and Mannich Bases in order to evaluate their potential as therapeutic options. All S1-9 and M1, 2, 4, and 7 molecules have molecular weights (mol MW) that are within acceptable ranges, with the exception of M7, M5, and M4. The factor QPPCaco, with a range of 92.279 to 347.271, was used to assess the permeability of such compounds. The Caco-2 cell permeability in nanometers per second, which is vital in assessing the permeability of biological membranes, is predicted by QPPCaco as a significant factor. The synthesized Schiff and Mannich Base compounds had partition coefficients (QPlogPo/w) in the range of 1.307 to 3.711, which are crucial for drug absorption and dispersion. The QPPMDCK values ranged from 46.861 to 335.935, and they indicated the anticipated apparent permeability in nanometers per second of MDCK cells. The estimated human oral absorption is represented by the% HOA values, which ranged from 72.581 to 90.709 on a scale from 0 to 100%. The QPlogS results also showed a 0.015 to -5.736 range in the water solubility. The Schiff and Mannich Base compounds developed for the novel satisfied all pharmacokinetics criteria for a drug-like substance, and the observed ranges were deemed therapeutically acceptable.
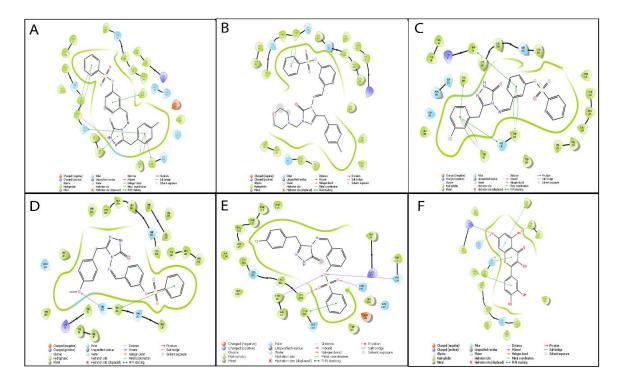
Fig. 1: 2D ligand interactions diagram of S5 (A), M5 (B), S8 (C), S6 (D), S7 (E), and positive control compound Quercetin (F) with AR receptor.
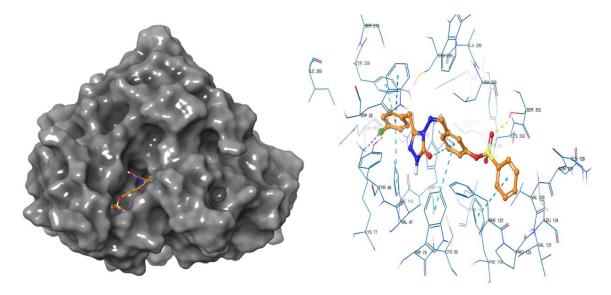

Fig. 2: 3D surfaced (left) and 3D detailed binding mode (right) of S7 compound.

Conclusion

The current study outlines the steps involved in the synthesis, structural analysis, and molecular docking research on newly created molecules. Nine recently found (Z)-3-[(3-substituted-5-oxo-1,5-dihydro-4H-1,2,4-triazol-4-yl)-iminomethyl] derivatives are included in the produced compounds.

Nine phenyl benzene sulfonates (S1-9) and five recently found (Z)-3-[(3-substituted-1-(morpholinomethyl)-5-oxo-1,5,dihydro-4H-1,2,4-triazol-4-yl)-iminomethyl] compounds are being investigated in this study. Phenyl benzene sulfonates, specifically **M1, 2, 4, 5, and 7**, are under consideration. The structures of the eight synthesized compounds were elucidated using ^{1}H NMR, ^{13}C NMR,

IR, and HR-MS spectroscopic techniques. This study investigated the inhibitory efficacy of benzenesulfonate derivatives on human recombinant AR. The findings obtained from the in vitro experiments suggest that compounds S1-9, M1, M2, M4, M5, and M7 exhibit significant inhibition of AR, with IC50 values spanning from 11.18 μM to 43.30 μM. These values are compared to the IC50 value of the quercetin compound, which is 5.68 μM. Among the substances studied, compound S7 showed the most promise as an androgen receptor inhibitor. Molecular docking, molecular mechanics, and ADME studies all supported the results of the experimental in vitro research. There is a considerable degree of correlation between the results of the computational simulations and the actual data. The main finding of this study suggests that using the S7 compound as the basis for the creation of novel aldose reductase inhibitors may be able to delay or prevent diabetic complications like neuropathy, nephropathy, retinopathy, and cataracts, which can have a negative impact on a person's quality of life.

References

1. S. Boy, A. Aras, F. Türkan, O. Akyıldırım, M. Beytur, H. Sedef Karaman, S. Manap, H. Yüksek, Synthesis, Spectroscopic Analysis, and in Vitro/in Silico Biological Studies of Novel Piperidine Derivatives Heterocyclic Schiff-Mannich Base Compounds, *Chem. Biodivers.*, **18,** (2021).

2. S. Boy, F. Türkan, M. Beytur, A. Aras, O. Akyıldırım, H.S. Karaman, H. Yüksek, Synthesis, design, and assessment of novel morpholine-derived Mannich bases as multifunctional agents for the potential enzyme inhibitory properties including docking study, *Bioorganic Chem.* **107**, (2021).

3. H. Medetalibeyoğlu, F. Türkan, S. Manap, E. Bursal, M. Beytur, A. Aras, O. Akyıldırım, G. Kotan, Ö. Gürsoy-Kol, H. Yüksek, Synthesis and acetylcholinesterase enzyme inhibitory effects of some novel 4,5-Dihydro-1H-1,2,4-triazol-5-one derivatives; an in vitro and in silico study, *J. Biomol. Struct. Dyn.*, **41**, (2022).

4. S. Sadeghian, L. Emami, A. Mojaddami, S. khabnadideh, Z. Faghih, K. Zomorodian, M. Rashidi, Z. Rezaei, 1,2,4-Triazole derivatives as novel and potent antifungal agents: Design, synthesis and biological evaluation, *J. Mol. Struct.*, **1271**, (2023).

5. F.S. Aljohani, O.A. Omran, E.A. Ahmed, E.S. Al-Farraj, E.F. Elkady, A. Alharbi, N.M. El-Metwaly, I. Omar Barnawi, A.M. Abu-Dief, Design, structural inspection of new bis(1H-benzo[d]imidazol-2-yl)methanone complexes:

6. Biomedical applications and theoretical implementations via DFT and docking approaches, *Inorg. Chem. Commun.*, **148**, (2023).

6. A.A. Al-Shamry, M.M. Khalaf, H.M.A. El-Lateef, T.A. Yousef, G.G. Mohamed, K.M.K. El-Deen, M. Gouda, A.M. Abu-Dief, Development of New Azomethine Metal Chelates Derived from Isatin: DFT and Pharmaceutical Studies, *Materials.*, **16**, (2022).

7. A.M. Abu-Dief, N.H. Alotaibi, E. S.Al-Farraj, H.A. Qasem, S. Alzahrani, M.K. Mahfouz, A. Abdou, Fabrication, structural elucidation, theoretical, TD-DFT, vibrational calculation and molecular docking studies of some novel adenine imine chelates for biomedical applications, *J. Mol. Liq.*, **365**, (2022).

8. X. Li, M. Lin, H. Zhang, W. Ji, Y. Shi, Z. Qi, T. Fu, Q. Li, Q. Deng, N-terminal epitope surface imprinted particles for high selective cytochrome c recognition prepared by reversible addition-fragmentation chain transfer strategy, *Chem. Pap.*, **76**, (2022).

9. A.M. Abu-Dief, R.M. El-khatib, F.S. Aljohani, S.O. Alzahrani, A. Mahran, M.E. Khalifa, N.M. El-Metwaly, Synthesis and intensive characterization for novel Zn(II), Pd(II), Cr(III) and VO(II)-Schiff base complexes; DNA-interaction, DFT, drug-likeness and molecular docking studies, *J. Mol. Struct.*, **1242**, (2021).

10. A. Das, G. Greco, S. Kumar, E. Catanzaro, R. Morigi, A. Locatelli, D. Schols, H. Alici, H. Tahtaci, F. Ravindran, C. Fimognari, S.S. Karki, Synthesis, in vitro cytotoxicity, molecular docking and ADME study of some indolin-2-one linked 1,2,3-triazole derivatives, *Comput. Biol. Chem.*, **97**, (2022).

11. H. Yüksek, Ö. Aktaş-Yokuş, Ö. Gürsoy-Kol, Ş. Alpay Karaoğlu, In-vitro biological activity of some new 1,2,4-triazole derivatives with their potentiometric titrations, *Indian J. Chem.*, **56B**, (2017).

12. M. Beytur, Fabrication of platinum nanoparticle/boron nitride quantum dots/6-methyl-2-(3-hydroxy-4-methoxybenzylidenamino)-benzothiazole (ILS) nanocomposite for electrocatalytic oxidation of methanol, *J. Chil. Chem. Soc.*, **65**, (2020).

13. M. Beytur, I. Avinca, Molecular, Electronic, Nonlinear Optical and Spectroscopic Analysis of Heterocyclic 3-Substituted-4-(3-methyl-2-thienylmethyleneamino)-4,5-dihydro-1 *H* -1,2,4-triazol-5-ones: Experiment and DFT Calculations, *Heterocycl. Commun.*, **27**, (2021).

14. R. Nithyabalaji, H. Krishnan, R. Sribalan, Synthesis, molecular structure and multiple biological activities of N-(3-methoxyphenyl)-3-

(pyridin-4-yl)-1H-pyrazole-5-carboxamide, *J. Mol. Struct.*, **1186**, (2019).

15. M.Z. Hassan, A. Alsayari, Y.I. Asiri, A.B. Muhsinah, 1,2,4-Triazole-3-Thiones: Greener, One-Pot, Ionic Liquid Mediated Synthesis and Antifungal Activity, *Polycycl. Aromat. Compd.* **43**, (2023).

16. N.H. Amin, M.T. El-Saadi, A.A. Ibrahim, H.M. Abdel-Rahman, Design, synthesis and mechanistic study of new 1,2,4-triazole derivatives as antimicrobial agents, *Bioorganic Chem.*, **111**, (2021).

17. H. Yüksek, A. Berkyürek, S. Manap, G. Özdemir, M. Beytur, H. Balseven, M. Alkan, F. Aytemiz, Ö. Gürsoy-Kol, Synthesis, characterization and investigation of antimicrobial and antioxidant activities of some new 2-[(4,5-dihydro-1H-1,2,4-triazol-5-one-4-yl)azomethine]phenyl 4-nitrobenzoate derivatives, *Indian J. Chem.*, **61**, (2022).

18. S. Tariq, P. Kamboj, O. Alam, M. Amir, 1,2,4-Triazole-based benzothiazole/benzoxazole derivatives: Design, synthesis, p38α MAP kinase inhibition, anti-inflammatory activity and molecular docking studies, *Bioorganic Chem.*, **81** (2018).

19. J. Ahirwar, D. Ahirwar, S. Lanjhiyana, A.K. Jha, D. Dewangan, H. Badwaik, Analgesic and Anti-inflammatory Potential of Merged Pharmacophore Containing 1,2,4-triazoles and Substituted Benzyl Groups via Thio Linkage, *J. Heterocycl. Chem.*, **55**, (2018).

20. E.D. Dincel, Ç. Akdağ, T. Kayra, E.D. Coşar, M.O. Aksoy, G. Akalın-Çiftçi, N. Ulusoy-Güzeldemirci, Design, synthesis, characterization, molecular docking studies and anticancer activity evaluation of novel hydrazinecarbothioamide, 1,2,4-triazole-3-thione, 4-thiazolidinone and 1,3,4-oxadiazole derivatives, *J. Mol. Struct.*, **1268**, (2022).

21. F. Kardas, S. Manap, Ö. Gürsoy-Kol, M. Beytur, H. Yüksek, Synthesis and antioxidant properties of some 3-Alkyl(Aryl)-4-[3-ethoxy-2-(4-toluenesulfonyloxy)-benzylidenamino]-4,5-dihydro-1H-1,2,4-triazol-5-ones, *Der Pharma Chemica*, **8**, (2016).

22. I. Saadaoui, F. Krichen, B.B. Salah, R.B. Mansour, N. Miled, A. Bougatef, M. Kossentini, Design, synthesis and biological evaluation of Schiff bases of 4-amino-1,2,4-triazole derivatives as potent angiotensin converting enzyme inhibitors and antioxidant activities, *J. Mol. Struct.*, **1180**, (2019).

23. İ. Küçükgüzel, E. Tatar, Ş.G. Küçükgüzel, S. Rollas, E.D. Clercq, Synthesis of some novel thiourea derivatives obtained from 5-[(4-aminophenoxy)methyl]-4-alkyl/aryl-2,4-dihydro-3H-1,2,4-triazole-3-thiones and evaluation as antiviral/anti-HIV and anti-tuberculosis agents, *Eur. J. Med. Chem.*, **43**, (2008).

24. He, X. Li, J. Li, X. Li, L. Guo, L. Hai, Y. Wu, A novel and convenient route for the construction of 5-((1H-1,2,4-triazol-1-yl)methyl)-1H-indoles and its application in the synthesis of Rizatriptan, *Tetrahedron Lett.*, **55**, (2014).

25. S. Varughese, Y. Azim, G.R. Desiraju, Molecular Complexes of Alprazolam with Carboxylic Acids, Boric Acid, Boronic Acids, and Phenols. Evaluation of Supramolecular Heterosynthons Mediated by a Triazole Ring, *J. Pharm. Sci.*, **99**, (2010).

26. J. Wen, K.A. Teske, M.K. Hadden, Inhibition of hedgehog signaling by stereochemically defined des-triazole itraconazole analogues, *Bioorg. Med. Chem. Lett.*, **30**, (2020).

27. Ł. Popiołek, A. Biernasiuk, K. Paruch, P. Patrejko, M. Wujec, Synthesis and evaluation of antimicrobial properties of new Mannich bases of 4,5-disubstituted-1,2,4-triazole-3-thiones, *Phosphorus Sulfur Silicon Relat. Elem.*, **192**, (2017).

28. G.L. Almajan, S.-F. Barbuceanu, E.-R. Almajan, C. Draghici, G. Saramet, Synthesis, characterization and antibacterial activity of some triazole Mannich bases carrying diphenylsulfone moieties, *Eur. J. Med. Chem.*, **44**, (2009).

29. Y. Zhang, Y.-Z. Zhan, Y. Ma, X.-W. Hua, W. Wei, X. Zhang, H.-B. Song, Z.-M. Li, B.-L. Wang, Synthesis, crystal structure and 3D-QSAR studies of antifungal (bis-)1,2,4-triazole Mannich bases containing furyl and substituted piperazine moieties, *Chin. Chem. Lett.*, **29**, (2018).

30. G. Hu, G. Wang, N. Duan, X. Wen, T. Cao, S. Xie, W. Huang, Design, synthesis and antitumor activities of fluoroquinolone C-3 heterocycles (IV): s-triazole Schiff–Mannich bases derived from ofloxacin, *Acta Pharm. Sin. B.*, **2**, (2012).

31. K. Buduma, N.K. A, S.S. KVN, K.K. J, S. Chinde, A.K. Domatti, Y. Kumar, P. Grover, A. Tiwari, F. Khan, Synthesis and bioactivity evaluation of eugenol hybrids obtained by Mannich and 1,3 dipolar cycloaddition reactions, *J. Heterocycl. Chem.*, **58**, (2021).

32. G. Jose, T.H.S. Kumara, H.B.V. Sowmya, D. Sriram, T.N.G. Row, A.A. Hosamani, S.S. More, B. Janardhan, B.G. Harish, S. Telkar, Y.S. Ravikumar, Synthesis, molecular docking, antimycobacterial and antimicrobial evaluation of new pyrrolo[3,2-c]pyridine Mannich bases, *Eur. J. Med. Chem.*, **131**, (2017).

33. E.V. Filho, M.K. Antoniazi, R.Q. Ferreira, G.F.S. dos Santos, C. Pessoa, C.J. Guimarães, J.B.V.

Neto, A.M.S. Silva, S.J. Greco, A Green Multicomponent Domino Mannich-Michael Reaction to Synthesize Novel Naphthoquinone-Polyphenols with Antiproliferative and Antioxidant Activities, *Eur. J. Org. Chem.*, **39**, (2022).

34. P. Alexiou, K. Pegklidou, M. Chatzopoulou, I. Nicolaou, V. Demopoulos, Aldose Reductase Enzyme and its Implication to Major Health Problems of the 21st Century, *Curr. Med. Chem.*, **16**, (2009).

35. S. Chung, S. Chung, Genetic Analysis of Aldose Reductase in Diabetic Complications, *Curr. Med. Chem.*, **10**, (2003).

36. C. Yabe-Nishimura, Aldose Reductase in Glucose Toxicity: A Potential Target for the Prevention of Diabetic Complications, *Pharmacol. Rev.*, **50**, (1998).

37. Y.L. Kao, K. Donaghue, A. Chan, J. Knight, M. Silink, A novel polymorphism in the aldose reductase gene promoter region is strongly associated with diabetic retinopathy in adolescents with type 1 diabetes, *Diabetes.*, **48**, (1999).

38. D.K. Moczulski, W. Burak, A. Doria, M. Zychma, E. Zukowska-Szczechowska, J.H. Warram, W. Grzeszczak, The role of aldose reductase gene in the susceptibility to diabetic nephropathy in Type II (non-insulin-dependent) diabetes mellitus, *Diabetologia*, **42**, (1999).

39. M. Brownlee, Biochemistry and molecular cell biology of diabetic complications, *Nature*, **414**, (2001).

40. V.F. Carvalho, E.O. Barreto, M.F. Serra, R.S.B. Cordeiro, M.A. Martins, Z.B. Fortes, P.M.R. e Silva, Aldose reductase inhibitor zopolrestat restores allergic hyporesponsiveness in alloxan-diabetic rats, *Eur. J. Pharmacol.*, **549**, (2006).

41. N. Hotta, T. Toyota, K. Matsuoka, Y. Shigeta, R. Kikkawa, T. Kaneko, A. Takahashi, K. Sugimura, Y. Koike, J. Ishii, N. Sakamoto, The SNK-860 Diabetic Neuropathy Study Group, Clinical efficacy of fidarestat, a novel aldose reductase inhibitor, for diabetic peripheral neuropathy: a 52-week multicenter placebo-controlled double-blind parallel group study, *Diabetes Care.*, **24**, (2001).

42. N. Hotta, Y. Akanuma, R. Kawamori, K. Matsuoka, Y. Oka, M. Shichiri, T. Toyota, M. Nakashima, I. Yoshimura, N. Sakamoto, Y. Shigeta, the ADCT Study Group, Long-Term Clinical Effects of Epalrestat, an Aldose Reductase Inhibitor, on Diabetic Peripheral Neuropathy: The 3-year, multicenter, comparative Aldose Reductase Inhibitor-Diabetes Complications Trial, *Diabetes Care.*, **29**, (2006).

43. R. Maccari, A. Del Corso, P. Paoli, I. Adornato, G. Lori, F. Balestri, M. Cappiello, A. Naß, G. Wolber, R. Ottanà, An investigation on 4-thiazolidinone derivatives as dual inhibitors of aldose reductase and protein tyrosine phosphatase 1B, in the search for potential agents for the treatment of type 2 diabetes mellitus and its complications, *Bioorg. Med. Chem. Lett.*, **28**, (2018).

44. L. Costantino, G. Rastelli, M.C. Gamberini, D. Barlocco, Pharmacological approaches to the treatment of diabetic complications, *Expert Opin. Ther. Pat.*, **10**, (2000).

45. S. Miyamoto, Molecular Modeling and Structure-based Drug Discovery Studies of Aldose Reductase Inhibitors, *Chem-Bio Inform. J.*, **2**, (2002).

46. S. Suzen, E. Buyukbingol, Recent Studies of Aldose Reductase Enzyme Inhibition for Diabetic Complications, *Curr. Med. Chem.*, **10**, (2003).

47. K.V. Ramana, Aldose reductase: new insights for an old enzyme, *Biomol. Concepts.*, **2**, (2011).

48. S.K. Srivastava, U.C.S. Yadav, A.B.M. Reddy, A. Saxena, R. Tammali, M. Shoeb, N.H. Ansari, A. Bhatnagar, M.J. Petrash, S. Srivastava, K.V. Ramana, Aldose reductase inhibition suppresses oxidative stress-induced inflammatory disorders, *Chem. Biol. Interact.*, **191**, (2011).

49. G. Kotan, H. Gökce, O. Akyıldırım, H. Yüksek, M. Beytur, S. Manap, H. Medetalibeyoğlu, Synthesis, Spectroscopic and Computational Analysis of 2-[(2-Sulfanyl-1H-benzo[d]imidazol-5-yl)iminomethyl]phenyl Naphthalene-2-sulfonate, *Russ. J. Org. Chem.*, **56**, (2020).

50. A.A. Ikizler, H. Yüksek, Reactions of ester ethoxycarbonylhydrazones with some amine type compounds, *Chim. Acta Turc.*, (1979).

51. A.A. Ikizler, H. Yüksek, Acetylation of 4-amino-44-dihydro-1H-1,2,4-triazol-5-ones, *Org. Prep. Proced. Int.*, **25**, (1993).

52. M.J. Cerelli, D.L. Curtis, J.P. Dunn, P.H. Nelson, T.M. Peak, L.D. Waterbury, Antiinflammatory and aldose reductase inhibitory activity of some tricyclic arylacetic acids, *J. Med. Chem.*, **29** (1986).

53. G. Madhavi Sastry, M. Adzhigirey, T. Day, R. Annabhimoju, W. Sherman, Protein and ligand preparation: parameters, protocols, and influence on virtual screening enrichments, *J. Comput. Aided Mol. Des,.* **27**, (2013).

54. W. Sherman, T. Day, M.P. Jacobson, R.A. Friesner, R. Farid, Novel Procedure for Modeling Ligand/Receptor Induced Fit Effects, *J. Med. Chem.*, **49**, (2006).

55. M. Sándor, R. Kiss, G.M. Keserű, Virtual Fragment Docking by Glide: a Validation Study

on 190 Protein−Fragment Complexes, *J. Chem. Inf. Model.*, **50**, (2010).

56. S. Genheden, U. Ryde, The MM/PBSA and MM/GBSA methods to estimate ligand-binding affinities, *Expert Opin. Drug Discov.*, **10**, (2015).

57. S. Kim, S. Hwang, H.-W. Suh, S. Lim, Phytochemical Analysis of Agrimonia pilosa Ledeb, Its Antioxidant Activity and Aldose Reductase Inhibitory Potential, *Int. J. Mol. Sci.*, **18**, (2017).

58. C. Nishimura, M. Furue, T. Ito, Y. Omori, T. Tanimoto, Quantitative determination of human aldose reductase by enzyme-linked immunosorbent assay: Immunoassay of human aldose reductase, *Biochem. Pharmacol.*, **46**, (1993).

59. K.E. Schemmel, R.S. Padiyara, J.J. D'Souza, Aldose reductase inhibitors in the treatment of diabetic peripheral neuropathy: a review, *J. Diabetes Complications.*, **24**, (2010).